Contrib Mineral Petrol (1983) 82:312–326

Contributions to Mineralogy and Petrology

Deformation and Related Radiochronology in a Late Pan-African Mylonitic Shear Zone, Adrar des Iforas (Mali)

J.R. Lancelot[1], A.M. Boullier[2], H. Maluski[3], and J. Ducrot[1]

[1] Laboratoire de Géochimie Isotopique et L.P. 361, and
[2] Equipe de Géologie du L.P. 361, and Present address: C.R.P.G., B.P. n° 20, F-54500 Vandœuvre les Nancy, France
[3] Laboratoire de Géologie Structurale et L.A. 266, Université des Sciences et Techniques du Languedoc Place Eugène Bataillon F-34060 Montpellier Cedex, France

Abstract. The influence of a deformation on the zircon U/Pb system was studied using the example of the western margin of the Iforas granulitic unit (Mali) where undeformed sub-alkaline leptynites have evolved to strongly foliated mylonites and then to ultramylonites. The deformation episod was late Pan-African and occurred at low temperature. Zircons show evidences of a brittle behavior with microcracks development, then, fracturation of the crystals and dispersion of the fragments in the ductile matrix. An equilibrium grain size was reached which probably depended of the stress, but was independant of the initial size of the zircons and of the strain.

In order to establish an accurate radiochronology of the studied area before the deformation, three rocks, not affected by the late Pan-African shear zone, have been dated by U/Pb method on zircons. In agreement to previous U–Pb, Rb–Sr and Sm–Nd data, the present results show that in the Iforas as in the western Hoggar, a main granulite facies metamorphism occurred 2,120±20 Ma ago. U/Pb data on zircons with inherited cores were interpreted by a multistage model with two episodic radiogenic lead losses, the first one at 2,120 Ma and the second one during Pan-African events. Then, a systematic investigation of the behavior of two chronometric systems (U/Pb on zircons and $Ar^{39}-Ar^{40}$ on feldspars) during a strong deformation episod at low temperature, was carried out. For the mylonitic episod, an upper limit of 566±8 Ma, is deduced from U/Pb data on non magnetic, coarse zircons of a late Pan-African granite, intruded in the western margin of the Iforas granulitic unit and slightly deformed by the mylonitic episod. Furthermore inherited cores are commonly present in these zircons, thus, the U/Pb data also indicated that this granite was formed 566±8 Ma ago, by partial melting of rocks with an apparent age of 2,609±200 Ma. A lower limit for the mylonitic episod was defined at 535±6 Ma by $Ar^{39}-Ar^{40}$ on K-feldspars extracted from a mylonite and an ultramylonite. An $Ar^{39}-Ar^{40}$ age of 900 Ma obtained on K-feldspars from an undeformed leptynite has no clear geological significance; the disturbing effect of the very closed shear zone, was probably not strong enough to reset totally the Ar chronometer. Finally, U/Pb data on zircons extracted from an ultramylonite indicated that the U–Pb system of these zircon fragments, remained closed during the deformation episod at low temperature.

The distinct behavior of the two radiochronological systems ($Ar^{39}-Ar^{40}$ on feldspars and U–Pb on zircons) is emphasized. For ultradeformed samples at low temperature, the age of the deformation and the age of the rocks which have undergone this deformation, can be determined using the two complementary chronometers.

Offprint requests to: J.R. Lancelot

I Introduction

Few studies have been undertaken concerning the opening of radiochronological systems as a function of deformation. Using Rb–Sr chronometers, Abbott (1972) has shown that $^{87}Sr/^{86}Sr$ homogenization can occur at the time of shearing over a volume of at least few square meters in a mylonite-bearing shear zone. Bernard-Griffiths (1975) reached the same conclusion for the Rb–Sr study of a mylonitized granite in the french Massif Central. The advantage of K-feldspar to date a tectonic event has been demonstrated by Maluski (1978) in a systematic study of the influence of deformation on the $Ar^{39}-Ar^{40}$ system of minerals. Numerous studies of the opening of a zircon U–Pb system during a thermal event have been made, but the relations between discordant U/Pb ages and deformation have never been investigated. A knowledge of discordance in the U–Pb system of zircons is essential for an understanding of the use of zircons in age-determination. The problem of discordant zircon ages has been treated as one of lead-loss in single stage models (Wetherill 1956; Tilton 1960; Wasserburg 1963; Ulrych 1963) and in multistage models (Allegre et al. 1974); it is usually assumed that episodic or continuous radiogenic lead-loss patterns (Pidgeon et al. 1966) are the result of thermal imprints on systems more or less susceptible to opening as a function of the degree of radiation damages. Nevertheless, Grünenfelder (1963) and Grünenfelder et al. (1968) proposed another mechanism involving chemical effects due to the presence of water in zircon crystals. More recently, Gebauer and Grünenfelder (1978) have suggested low-temperature recrystallization of zircon as a cause of discordant U/Pb data.

Several cases of contact metamorphism (Gastil et al. 1967; Davis et al. 1968), middle and high-grade metamorphism (Grauert 1974) have been studied in detail for the U–Pb dating of zircon. On the other hand, the lack of studies of the relation between deformation and zircon-ra-

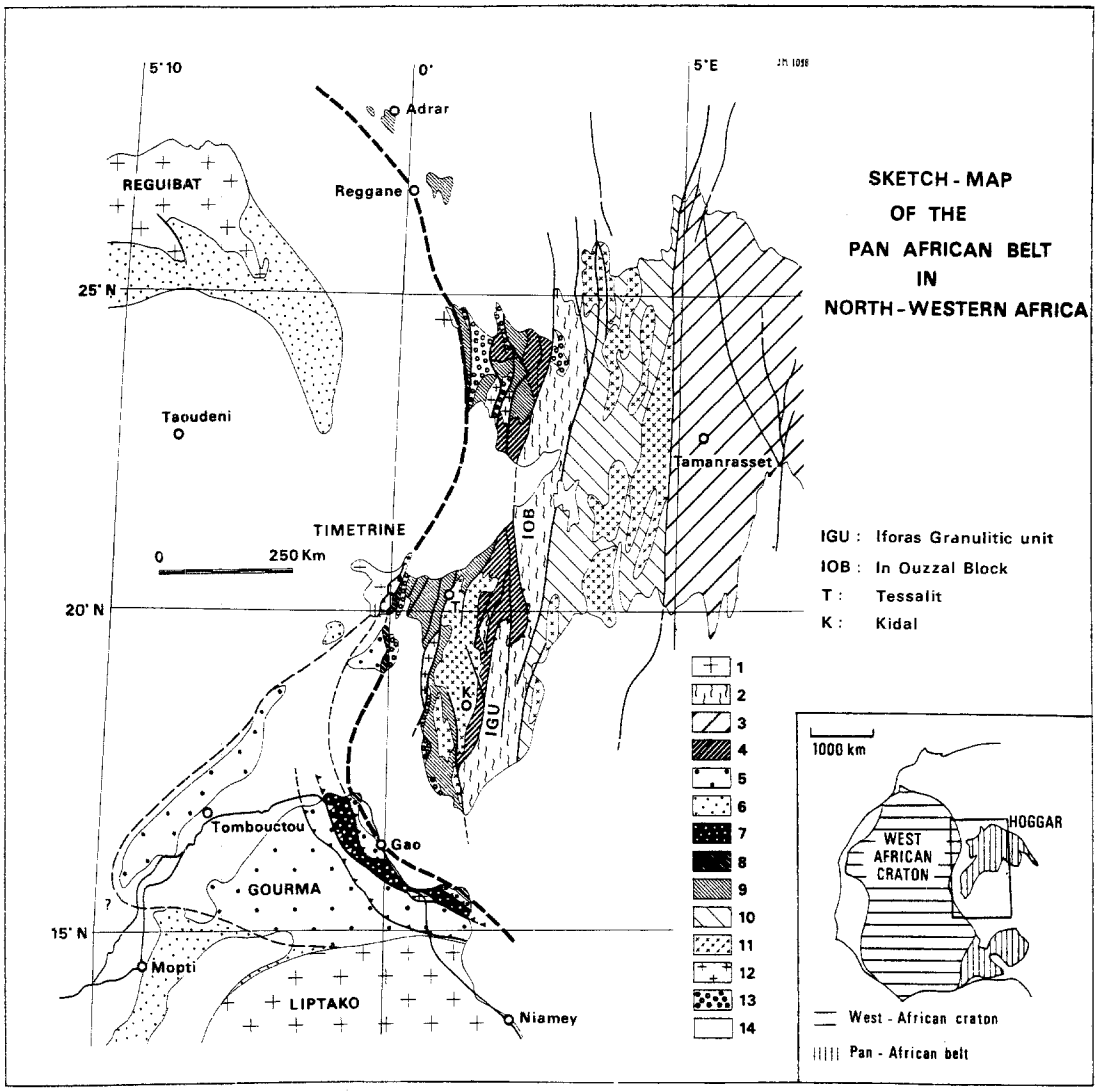

Fig. 1. Sketch-map of the Pan-African mobile belt in north western Africa (after Bertrand et al. 1980). (1) West-African craton: Eburnean basement (2) Eburnean basement slightly reactivated with its sedimentary cover of the middle to upper Proterozoic age (3) Central polycyclic Hoggar: Eburnean reworked material (4) Eburnean basement and its middle to upper Proterozoic cover highly deformed and metamorphosed during the Pan-African event (5) Upper Proterozoic deformed sediments of the Gourma aulacogene and of the Timetrine nappes (6) Upper Proterozoic tabular sediments of the Taoudeni basin (7) Internal nappes the Gourma (HP/BT Pan-African metamorphism) (8) Ultrabasic rocks of the suture (9) Accretion zone: upper Proterozoic volcanoclastics and intrusives (10) Upper Proterozoic volcanic sedimentary series of the eastern branch of the Pan-African chain (11) Pan-African granitoids (12) Formations showing HT/BP Pan-African metamorphism (13) Post Pan-African molasse (14) Post Cambrian cover. Discontinuous thick line: suture zone

diochronology is remarkable. As a matter of fact, previous U/Pb systematic dating of the basement of western and central Africa (Lancelot et al. 1973, 1976; Lancelot 1975; De la Boisse and Lancelot 1977; Desportes and Lancelot 1975) indicated that zircons of the same age, of similar U content and the same thermal history show different degrees of discordance, possibly correlated to the intensity of zircon fracturing during thermo-tectonic events. To investigate the behavior of zircon U/Pb system, during a strong deformation episod at low temperature, we choised the case of the western mylonitic margin of an Eburnean granulitic unit in the Adrar des Iforas (Mali). The shear zone is late Pan-African, thus in this case study, the deformation gradient occurred a long time (1,400–1,500 Ma) after the crystallization or the recrystallization of zircon in granulite facies metamorphism.

II Geological Setting

II.1 The Iforas Granulitic Unit and Its Pan-African Reworking

The Pan-African mobile belt (Fig. 1) is assumed to be the result of the collision of two continental margins: the West-African craton and an eastern block (Black et al. 1979; Bertrand et al. 1980; Caby et al. 1981) where an Eburnean basement and its sedimentary cover of Proterozoic age were deformed together during the Pan-African events (Caby 1970; Allègre and Caby 1972; Clauer 1976). In this domain, the Iforas granulitic unit is considered to be equivalent to the In Ouzzal block in Algeria (Caby and Boullier 1977; Boullier et al. 1978). Radiochronological studies of this block indicate that the granulite metamorphism occurred

2,120 ± 50 my ago and affected the material of a 3,100–3,300 my old continental crust. These conclusions are deduced from U–Pb studies of zircons (Lancelot et al. 1973, 1976; Lancelot 1975) and recent Rb–Sr and Sm–Nd measurements performed on whole rocks and separate minerals (Allègre and Ben Othman 1980).

The Iforas granulitic unit is composed of:

1. Metasedimentary rocks, various banded gneisses, mostly quartzites and semipelitic gneisses, which show a typical mineralogical association of the granulite facies. As in the Ouzzal granulitic unit (Leyreloup 1974) the high-pressure mineral associations (garnet, hypersthène, sillimanite, rutile) are partly overprinted by medium-pressure and high-temperature ones (cordierite, biotite, hypersthene). No evidence of a structural break can be found between the two stages, which are believed to belong to the same granulitic event (Caby and Boullier 1977).

2. Sub-alkaline leptynites: they constitute the greatest part of the Iforas granulitic unit. It is a monotonous banded formation whose layering is defined by variations in mineral percentage: quartz, mesoperthite, clinopyroxene ± amphibole ± biotite. The formation has been migmatized, as demonstrated by the quartzo-feldspathic veins which are parallel to or cross-cut the banding of the leptynites. The migmatization took place during the high temperature granulitic event (granitic to alkali-granitic composition precludes the presence of orthopyroxene). The origin of the leptynites is not clear, since their banding is concordant with that of the metasediments. In fact they could represent either a thick monotonous metavolcanic formation or early alkaline intrusives.

3. Eburnean intrusive rocks. These are of three kinds: meta-ultrabasic rocks, norites and charnockites. The latter were syntectonically emplaced during the last N 60 phase of Eburnean orogenesis or slightly postdate it.

The Pan-African reworking of the Iforas granulitic unit is localized in certain narrow zones:

- pre-tectonic basis dykes cutting all the preexisting Eburnean structures and the Upper-Proterozoic cover of the granulites;
- mylonites due to early thrusting on the northern and eastern margins and in certain narrow internal shear zones (Boullier et al. 1978; Boullier 1980a);
- metamorphism of epidote-amphibolite facies grade;
- intrusion of Pan-African granites;
- and late mylonitization of the western margin (Boullier 1980b). This mylonitized margin, which is a shear zone, will be our main interest.

The western mylonitic margin of the Iforas granulitic unit is a very straight NO 10 trending shear zone and can easily be seen on ERTS photographs. It is a 300 km-long structure which sharply cross-cuts the banding of granulites and also a late Pan-African calc-alkaline granite. This granite intrudes the Iforas granulitic unit (Fig. 2), and has been dated in this work with the U/Pb method on zicons. The main unit, which is deformed by this shear zone, is a homogeneous formation of sub-alkaline leptynite.

In the field, evolution of strain is very clear and all the stages can be observed. The shear zone is defined by a strong penetrative mylonitic foliation which is vertical and bears a horizontal stretching lineation. A strain gradient 500 m wide is observed. Assuming that the stretching lineation is the movement direction, we way interpret this shear zone as a strike-slip fault with a probable sinistral

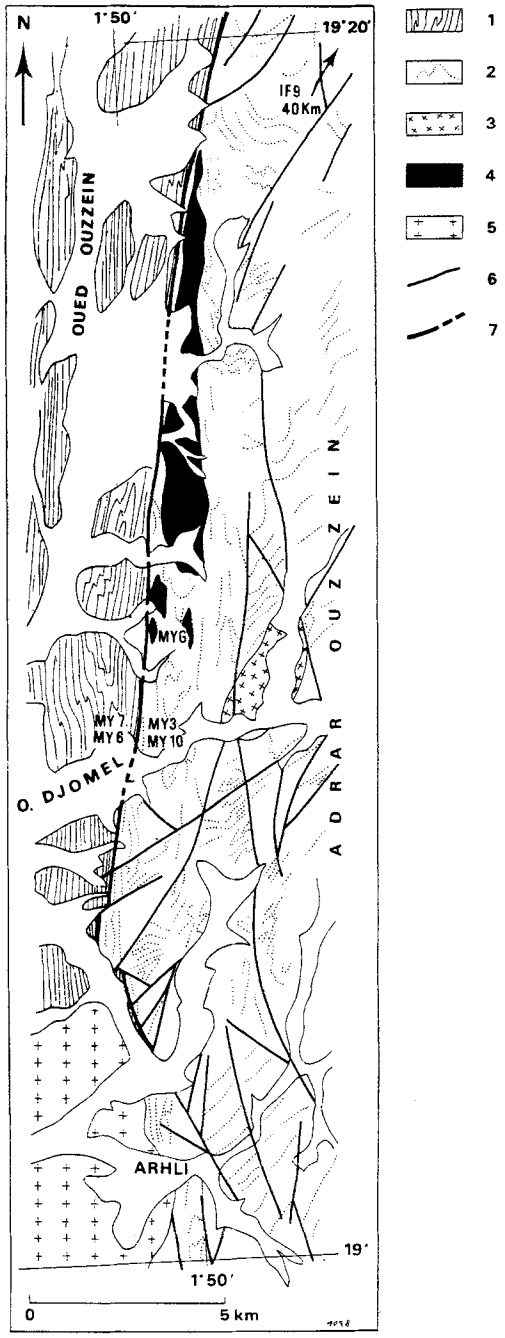

Fig. 2. Schematic map of the shear zone: (1) Gneissic rocks in the amphibolite facies (2) Eburnean granulites (3) Eburnean charnockitic granitoids (4) Pan-African granite (MYG) pretectonic of the shear zone (5) Pan-African granite post tectonic of the shear zone (6) Fault (7) Shear zone

movement. This fault separates the Iforas granulitic unit from the polycyclic gneisses of the West, where evidence of shearing, together with compression, may also be related to the shear zone.

II.2 The Gradient of Strain in the Shear Zone

Our study focuses on an area where the leptynites show homogeneous mineral content and where the gradient of strain is clear: the Adrar Ouzzein (Fig. 2). We describe only one half of the shear zone (the eastern one) since the other

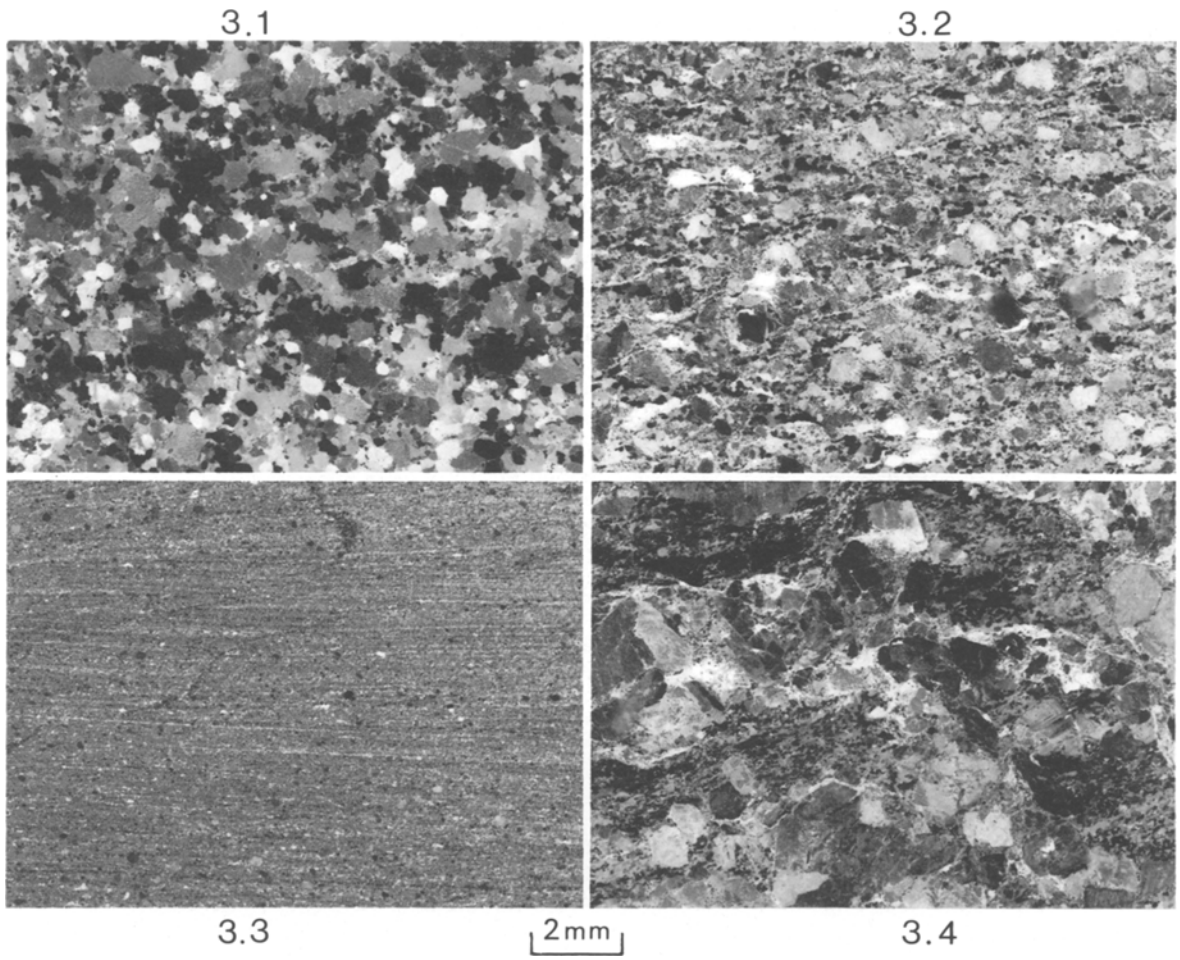

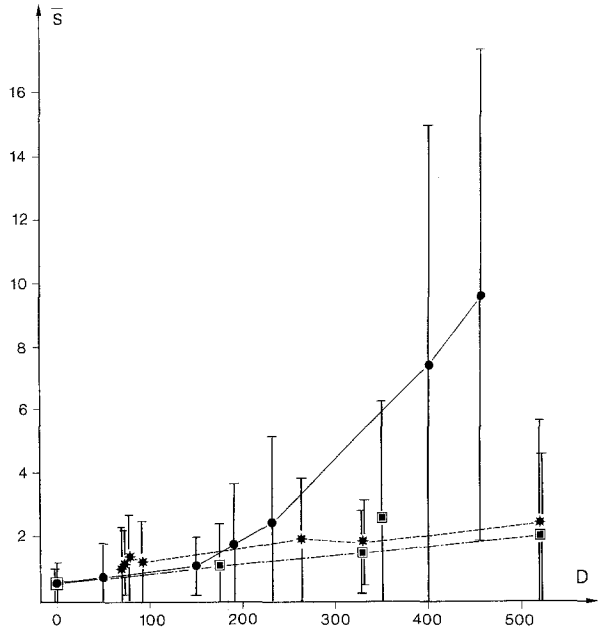

Fig. 3. 3.1, 3.2, 3.3: Photographs of granulitic gneisses showing different states of strain due to the Pan-African deformation in the shear zone. Scale bar: 2 mm; negative prints; crossed nicols. Note the decreasing grain size with increasing strain (3.1 to 3.3).
3.1: corresponds to undeformed samples and 3.3 to one sample taken in the center of the shear zone;
3.4: Photograph of the pretectonic (in respect to the mylonitisation) Pan-African granite (MYG).
Average surface of zircons measured in thin sections ($\bar{S}$ in 10^2 μ^2) versus the distance (D in meters) of the sample to the center of the shear zone; 30 to 60 grains have been measured for each sample. Different symbols (solid points, squares and stars) correspond to three parallel cross-sections of the shear zone (Boullier 1980)

part involves heterogeneous polycyclic gneisses with complex structures. The undeformed leptynites are banded and brownish in color and consist of 30% to 50% blue quartz. Further toward the shear zone (less than 500 m) the quartz becomes milky; the feldspar pink, and a new vertical foliation appears, cross-cutting the preexisting banding. It is defined by the flattening of quartzo-feldspathic lenses and green amphibole. With increasing strain, the layering of the leptynites is no longer recognizable. The lenses of quartz and feldspar become more and more flattened and finally form fine-grained vertical narrow mylonitic banding. The horizontal stretching lineation is defined by the elongation

of quartz and feldspar which from ribbons, and by the orientation of green amphibole, and by strings of small greenish biotite and ore minerals (magnetite – ilmenite). In the center of the shear zone, the ultramylonites have a very fine grain-size and some folds give a fluidal aspect to the rocks. But the mylonitic foliation always forms the axial plane and the stretching lineation corresponds to the axis of these folds. So, like Quinquis et al. (1978), we assume that these structures were produced by high shearing during a progressive deformation.

II.3 Structures in Thin Section

The undeformed leptynites are coarse-grained (1 or 2 mm in average, Fig. 3.1). No flattening of the primary minerals is evident, except for the layering defined by differences in percentage or in size of minerals (quartz, mesoperthite, plagioclase, clinopyroxene, opaque and accessory minerals). The texture is inequigranular granoblastic (Collerson 1974). Even in the undeformed rocks, we find some signs of slight strain: the quartz grains show undulatory extinction, prismatic substructures, and lobate quartz-quartz grain boundaries but dynamic recrystallization occurs very rarely (less than 1% in volume). The other minerals (clinopyroxene and feldspars) do not show any evidence of plastic deformation, but some cracks appear where tiny needles of green amphibole develop, or which are filled by calcite. In the first stage of deformation (protomylonites, Higgins (1971) and Sibson (1977) a penetrative foliation appears. It is characterized by the flattening of quartz lenses, strings of green amphibole which grow syntectonically from relicts of pale green clinopyroxene, and by the stretching of opaque minerals. Quartz grains are almost entirely polygonized and a mosaic of small equant crystals ($\simeq 100$ μ in diameter) replaces the highly-deformed porphyroclasts. In actual fact, this recrystallization coincides with the change of colors in quartz from blue to milky.

The plastic behavior of quartz contrast with the brittle behavior of other minerals such mesoperthite, zircon, and apatite in which cracks are very common. Between two fragments of mesoperthite, the cracks are filled with quartz and very small grains of albite (20 μ in diameter). This, again, underlines the important role of strain in the diffusion and repartition of elements in metamorphic rocks.

In the mylonitic rocks, foliation is continuous and defines a tectonic banding (Fig. 3.2). Quartz forms ribbons constituted by an equant mosaic of grains with constant size (100 μ). They are deflected by the porphyroclasts of mesoperthite which partly recrystallize into albite on their boundaries and form augen. Opaque minerals, fractured zircons, and apatites are dispersed and then form strings of isolated grains. In these rocks, temperature decrease during the deformation since the green amphibole is partly replaced by greenish biotite, and calcite grains appear in the feldspathic layers. The structure of the granite involved in the shear zone is comparable to that of the mylonites except for the nature of feldspars.

In the center of the shear zone, the leptynites are ultramylonitized and the average grain size is very small (about 20 μ) except for some relicts of mesoperthite which still remain and allow us to recognize the original granulitic material (Fig. 3.3). At this stage of very high strain, the amphibole is entirely replaced by greenish biotite which is itself partly chloritized. Grains of calcite are dispersed between the other minerals. The mineral phases no longer define a clear tectonic layering but are mixed together. This fact, together with other characteristics of the ultramylonites – high strain, very fine grained crystals, no preferred lattice-orientation at least for quartz – are compatible with a superplastic flow as suggested by Boullier and Gueguen (1975) for some mylonites.

II.4 Behavior of Zircons

The main feature of these mylonitic rocks is the decrease in grain-size toward the center of the shear zone (Fig. 3). Some measurements have been done on zircons which have brittle behavior and are not subject to dynamic recrystallization at low temperature (Boullier 1980b). As soon as the protomylonitic foliation appears, cracks are formed in zircon and the grain-size decreases until an equilibrium grain-size is obtained. Then the grains are passively rolled and dispersed in the ductile matrix and this equilibrium grain-size does not change (or only a little) even with increasing strain. This size is also the same for the three sections across the shear zone and is probably dependent on the parameters of deformation (stress). The mesoperthites have a similar behavior (Boullier 1980b).

III Experimental Procedures

III.1 Zircon U–Pb Dating

Several zircon fractions were extracted from each studied sample, of which 3 to 10 kg were crushed and mechanically separated into fractions of various sizes, each of which was split into several fractions by heavy liquids and magnetic separation. All samples were handpicked to reduce impurities, then cleaned for 30′ in warm HNO_3 8 N and in HCl 6 N successively and put in an ultrasonic cleaner with tridistillated H_2O and dried. 1 to 3 mg of zircon was placed in the 150 μl chamber of a PTFE microbomb (Lancelot 1975).

After the addition of HF, the microbomb was closed, squeezed with a thermo-shrinkable FEP tube, and put in a stainless steel container, with PTFE gaskets. Generally dissolution was obtained after 60–70 h, at 200° C, using 50 μ isothermally pentadistilled HF. Chemical separation on an ion exchange resin and evaporation to dryness were done in a vertical laminar flow hood. For Pb and U purification, a method of anion resin columns was applied, as introduced by Krogh (1973). Measurements of the isotopic ratios were performed on a solid-source mass spectrometer CAMECA TSN 206 S equipped with programmed magnetic field and one-line digital data acquisition and processing, using a TI 360 A computer and a Silent ASR 700 unit. Silicagel purified by HBr 1 N and concentrated HNO_3 were used for Pb analysis (Tatsumoto, personal communication). Sample was loaded on an ultrapure M-shaped rhenium filament ($e=25$ μ). For "concentration" runs, both spiked Pb and U were loaded on the same M shape filament together with silicagel. Lead emits at temperatures ranging from 1,200° C to 1,400° C, while the uranium emission as UO_2 beam occurs from 1,400° C to 1,550° C (Lancelot et al. 1979). Total blanks measured during the period of analysis, ranged from 0.3 to 0.1 10^{-9} g for the lead; the measured isotopic composition of the common lead from pollution was $^{206}Pb/^{204}Pb=18.10$, $^{207}Pb/^{204}Pb=15.49$ and $^{208}Pb/$

Table 1. U–Pb Analytical Datas of Zircons

Sample grain size (micron)		Sample weight (10^{-3} g)	U (ppm)	Radiogenic Pb (ppm)	Observed $^{206}Pb/^{204}Pb$	$^{206}Pb/^{238}U$	$^{207}Pb/^{235}U$	$^{207}Pb/^{206}Pb$
Quartzite M578 – In Ouzzal								
50–63	+	2.54	538	206	4,043	0.3652	6.6105	0.13136
50–63	+	2.95	548	216	4,965	0.3766	6.8376	0.13168
50–63	–	2.72	526	181	9,360	0.3282	6.0104	0.13282
50–63	++	2.65	552	218	5,214	0.3712	6.7521	0.13193
Leptynite MY3 – Iforas								
125–150	+	2.40	632	227	2,316	0.32612	6.4868	0.14426
100–125	+	2.58	635	220	1,913	0.31561	6.2004	0.14247
80–100	+	2.18	622	219	2,598	0.32137	6.3260	0.14276
63–80	+	2.45	569	203	2,797	0.32526	6.4059	0.14284
125–150	–	2.45	346	135	7,089	0.35187	7.2739	0.14992
100–125	–	2.57	367	156	6,877	0.38186	8.0185	0.15229
80–100	–	2.48	313	135	10,929	0.38989	8.1399	0.15141
63–80	–	2.18	282	127	8,049	0.40914	8.5380	0.15134
Quartzite IF9 – Iforas								
150–200	±	1.08	384	162	10,996	0.37868	8.0185	0.15357
125–150	±	2.03	422	177	13,229	0.38682	7.6428	0.14329
100–150	±	2.42	317	124	6,529	0.35345	7.1839	0.14740
80–100	±	2.40	322	122	12,352	0.35140	6.9138	0.14269
63–80	±	2.34	348	133	12,052	0.35727	7.0031	0.14216
100–125	+	1.48	276	104	10,453	0.34456	6.8610	0.14442
63–80	+	1.36	311	115	5,206	0.34661	6.6838	0.13985
Granite MYG – Iforas								
Opaque	63–80 +	1.66	595	51.7	1,020	0.08485	0.73871	0.06314
Clear	63–80 –	1.86	786	70	1,427	0.08715	0.74979	0.06239
Mix	63–80 ±	2.17	666	59.6	737	0.08749	0.76916	0.06375
Opaque	80–100 +	2.10	661	60.5	1,131	0.08922	0.81242	0.06603
Clear	80–100 –	2.29	888	80	1,537	0.08884	0.76927	0.06279
Mix	80–100 ±	2.32	668	61	1,075	0.08914	0.79005	0.06427
Clear	125–150 –	0.95	481	48	1,437	0.09614	0.8669	0.06539
Mix	100–125 ±	0.82	574	59	1,488	0.09881	0.94447	0.06932
Mix	125–150 ±	2.67	583	62	1,093	0.10269	1.05367	0.07441
Mix	150–200 ±	1.18	866	96	1,423	0.10732	1.17273	0.07925
Ultramylonite MY7 – Iforas								
125–150	±	0.16	332	125	1,384	0.35163	6.28533	0.12964
100–125	±	0.16	728	282	2,527	0.36352	6.52934	0.13023
80–100	±	0.90	444	171	2,300	0.36630	6.61025	0.13088
63–80	±	1.31	475	182	1,764	0.35857	6.44966	0.13046

(++): hightly magnetic; (+): magnetic; (–): non magnetic; (±): magnetic + non magnetic
Measured isotopic composition of the common lead of pollution: $^{206}Pb/^{204}Pb = 18.2$; $^{207}Pb/^{204}Pb = 15.5$; $^{208}Pb/^{204}Pb = 38.5$

$^{204}Pb = 39.50$. Using 982 NBS standard, a systematic measurement of mass discrimination was performed and this indicated a constant mean mass discrimination of 0.12% per mass unit during lead runs in the mass spectrometer (Cogez and Sulmont 1978). The decay constants of uranium were taken as $\lambda_8 = 0.155125.10^{-9}\, a^{-1}$ and $\lambda_5 = 0.98485.10^{-9}\, a^{-1}$ and the ratio $^{238}U/^{235}U$ as 137.88 (Jaffey et al. 1971; Steiger and Jäger 1977). Isotopic results are given with 95% percent confidence limit errors and error correlation calculated according to Ludwig (1980).

III.2 Feldspar $A^{39}-A^{40}$ Dating

Samples were purified with a Frantz magnetic separator. A mixture of K-feldspars, plagioclase and quartz was then put into $CHBr_3$, which was progressively diluted in order to obtain pure K-feldspar (>98%) in the last fraction. Samples were cleaned with an ultrasonic vibrator and transferred to a sealed quartz vial. Minerals were irradiated in the Melusine reactor (CENG, Grenoble) which delivers a flux of $1.4.10^{13}$n/cm^2/s. Five samples were irradiated for 24 h in one container with a monitor (Biotite 3 MAL 1 (Albarède 1971)) and were arranged in a crown in order to receive an equivalent flux of fast neutrons. Samples were kept a minimum of 15 days after irradiation. Each sample was wrapped in nickel foil, heated and then fused in a molybdenum crucible. Released gas was purified on a Zr–Al getter at 400° C. Spectrometric analyses were carried out on a THOMSON-CAMECA 205 E ultra-modified spectrometer. In order to correct for mass interferences, pure K_2SO_4 and CaF_2 salts were analyzed. Measurements of $^{40}Ar/^{36}Ar$ yielded an average of 293. Discrimination correc-

Table 2: Argon analytical data of feldspars

Step	Temp. (°C)	$^{40}Ar/^{39}Ar$	$^{36}Ar/^{39}Ar$	$^{37}Ar/^{39}Ar$	$^{40}Ar^*/^{39}Ar$	Age (Ma)	% ^{39}Ar (by step)
MY6A K-Feldspar							
1	635	41.58	0.034	0.0	31.458	438.0±11.8	1.206
2	760	36.99	0.004	0.011	35.703	490.0± 9.5	11.370
3	870	39.59	0.001	0.0	39.230	532.1±10.2	28.717
4	970	38.84	0.002	0.0	39.071	530.2±10.3	14.693
5	1,075	39.99	0.001	0.0	39.490	535.1±10.1	21.949
6	1,175	41.69	0.003	0.0	40.595	548.2±11.9	11.940
7	1,240	48.78	0.002	0.0	48.011	633.1±12.4	9.062
8	1,340	68.31	0.057	0.0	51.206	668.6±17.3	0.714
9	1,575	162.8	0.305	0.0	72.467	889 ±42.7	0.349
MY10 K-Feldspar							
1	635	59.78	0.058	0.0	42.287	569.1±16.7	0.457
2	760	38.77	0.021	0.0	32.482	450.6±11.2	0.898
3	870	38.14	0.007	0.0	36.096	494.7±10.4	2.712
4	970	39.01	0.005	0.0	37.558	512.3±10.6	5.286
5	1,075	39.78	0.005	0.0	38.342	521.6±11.8	6.069
6	1,175	38.68	0.003	0.0	37.605	512.8±11.0	9.043
7	1,246	41.15	0.003	0.0	40.225	543.8±11.1	8.031
8	1,340	38.87	0.003	0.0	37.816	515.3±10.0	10.176
9	1,435	39.20	0.003	0.0	38.137	519.2±10.7	13.202
10	1,470	41.01	0.004	0.002	39.775	538.6±11.9	18.030
11	1,500	40.94	0.005	0.0	39.286	532.8±11.5	15.960
12	1,575	40.67	0.007	0.0	38.487	523.9±11.5	10.137
MY3 K-Feldspar							
1	635	64.26	0.012	0.0	60.772	770.4±15.2	1.656
2	760	46.27	0.007	0.0	44.022	589.0±12.1	2.950
3	870	44.17	0.003	0.004	43.095	577.3±11.0	5.956
4	970	45.60	0.003	0.004	44.570	594.2±11.1	6.178
5	1,075	46.07	0.002	0.003	45.373	603.4±12.8	6.044
6	1,175	50.85	0.002	0.003	50.317	658.8±13.1	10.990
7	1,240	53.82	0.001	0.003	53.476	693.4±13.3	14.350
8	1,575	72.98	0.004	0.007	71.930	883.7±13.5	51.870

$\lambda = 5.54 \cdot 10^{-10}\ a^{-1}$
All ratios corrected for neutron induced interferences (for correction parameters: see Maluski 1978).
40 Ar* is radiogenic argon $(^{40}Ar^*/^{39}Ar)_M = 21.49$

tion was carried out with this value. In this work the J value of the monitor was equal to $(e^{\lambda T}-1)/(^{40}Ar^*/^{39}Ar)$ with $\lambda = 5.54\ 10^{-10} a^{-1}$ and $T = 310 \pm 5$ Ma.

IV Regional Geochronological Background: The Granulite Facies Metamorphism in the Western Hoggar and the "Adrar des Iforas"

Previously to a systematic investigation of the behavior of two chronometric systems (U/Pb on zircons and Ar^{39}/Ar^{40} on feldspars) during a strong deformation episod at low-temperature, it was necessary to define the age of the rock ulteriorly deformed. This rock was a subalkaline leptynite (described part II) from the Iforas granulitic unit; thus, to define the age of the granulite facies metamorphism in the Iforas and compare with that of the In Ouzzal granulitic unit, two quartzites and one undeformed leptynite were analyzed by U/Pb on zircons.

IV.1 Quartzite M578 from the In Ouzzal Granulitic Unit

The quartzite M578 of the In Ouzzal granulitic unit does not show zircons with inherited cores; zircons M578 are abundant, clear, round (drop-shaped), colorless, without inclusion (Fig. 4); these zircons of small size (30 μ in average diameter) show a high degree of purity; trace elements cannot be detected with electron microprobe in these crystals. They show all the characters of zircons which have crystallized under conditions of high pressure metamorphism (see the discussion of this point in Lasnier (1977), p. 128–131, and in Hope (1966)). Slightly discordant, the experimental points corresponding to these zircons define a linear array whose upper intercept with the Concordia curve, indicates an age of 2,115±6 Ma (Fig. 5), which is well in agreement with previous U–Pb data obtained with zircons from charnockite gneiss M408, sampled from the same unit (Lancelot et al. 1973, 1977; Lancelot 1975). Thus, the occurrence of a 2,115 Ma granulite metamorphism in the In Ouzzal granulitic unit is well established. The tectonic and metamorphic reworking of this unit during Pan-African orogeny seems to have been weak (Caby 1970).

IV.2 Undeformed Sub-Alkaline Leptynite MY3 of the Iforas Granulitic Unit

Abundant, clear, rounded, brownish to reddish zircons, with a common ovoidal shape and pseudo faces (Fig. 4)

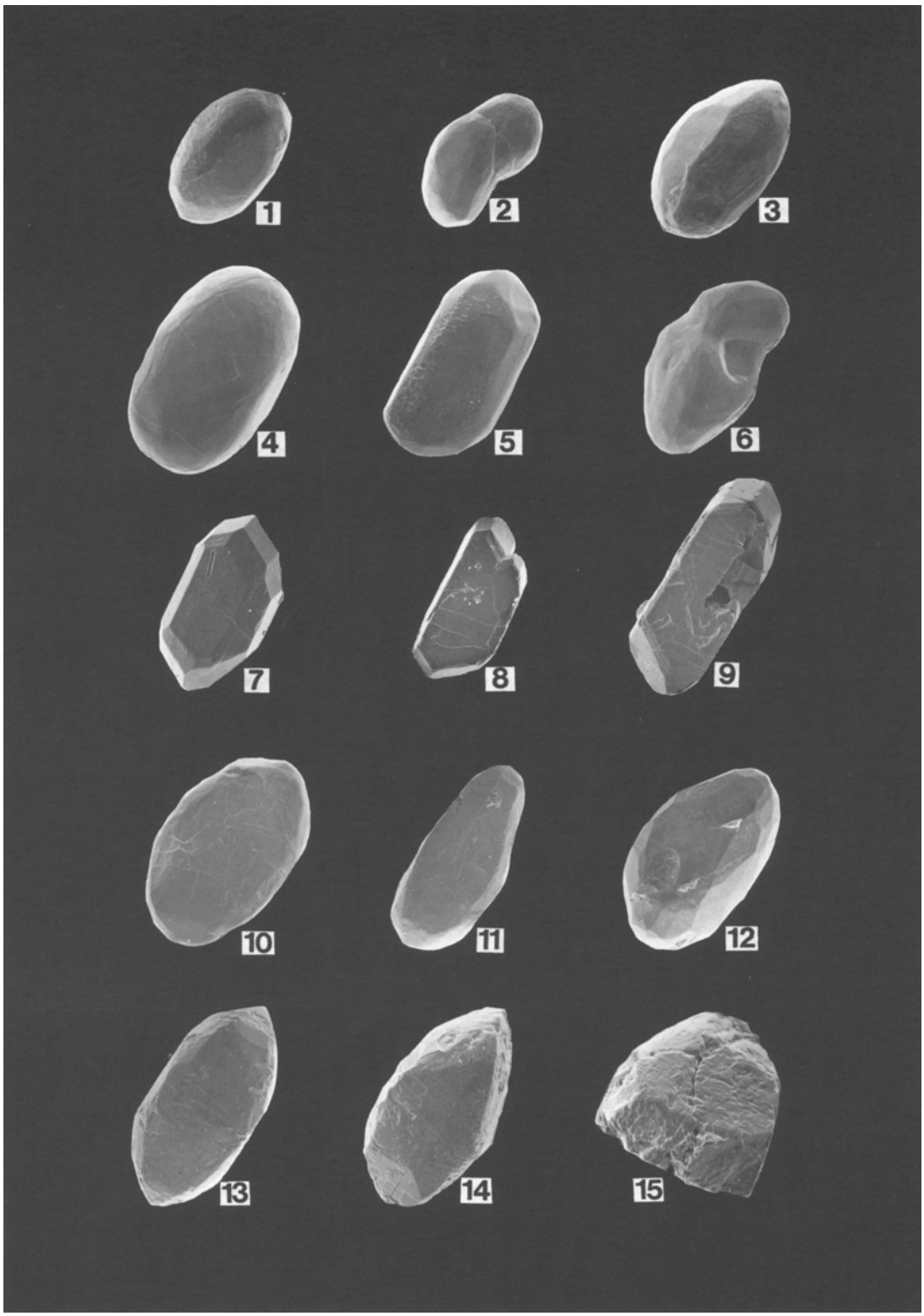

Fig. 4. (1) ×1,000, (2) ×800, (3) ×1,000, zircons from the quartzite M578, (4) ×600, (5) ×460, (6) ×460, zircons from the quartzite IF9; crystallized under H.P. metamorphism, these small crystals are rounded (drop-shaped) and characterized by the development of pseudo-faces. (7) ×400, (8) ×320, (9) ×360 euhedral zircons of the late Pan-African granite MYG deformed by the studied shear zone. Note microcracks development and the common association of two of more crystals following the C axis (see also Fig. 8). (10) ×300, (11) ×200, (12) ×300, rounded zircons from the undeformed leptynite MY3; note the extensive development of microcracks even in the undeformed sample. Zircons show ovoidal shapes and pseudo faces, common characters of zircons crystallized under H.P. metamorphism, (13) ×720, (14) ×720, (15) ×780, zircons from the ultramylonite MY7; note the strong superficial corrosion and the breackage of crystals during the mylonitic episod. In this ultramylonite, zircons are commonly reduced to fragments well represented by the microphotograph (15)

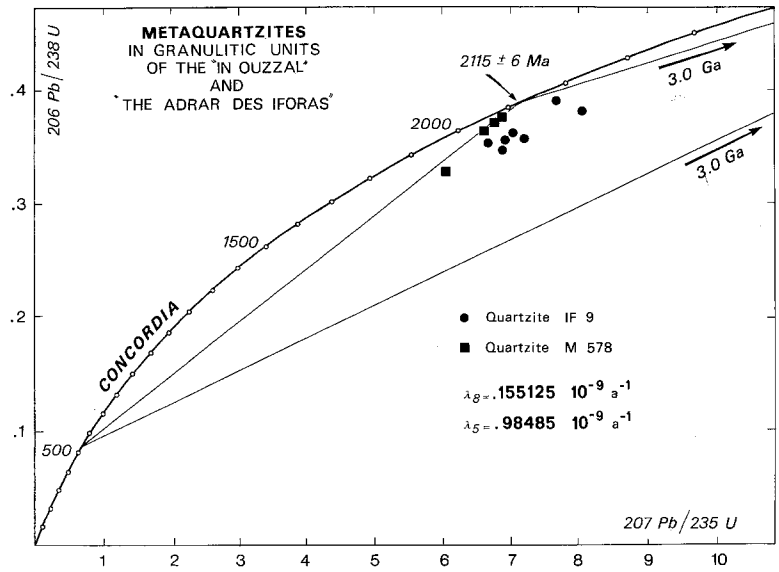

Fig. 5. Concordia diagram $^{207}Pb/^{235}U$ vs $^{206}Pb/^{238}U$, for zircons of the quartzites M578 (In Ouzzal granulitic unit) and IF9 (Iforas granulitic unit). A two stages model is assumed for zircons IF9: a primary discordance was produced during the 2,115 Ma metamorphism on U/Pb system of detrital zircons inherited from a basement 3.0–3.3 Ga old, a secondary discordance was developed through the main Pan-African metamorphic event (550–650 Ma in the studied area) or late Pan-African events

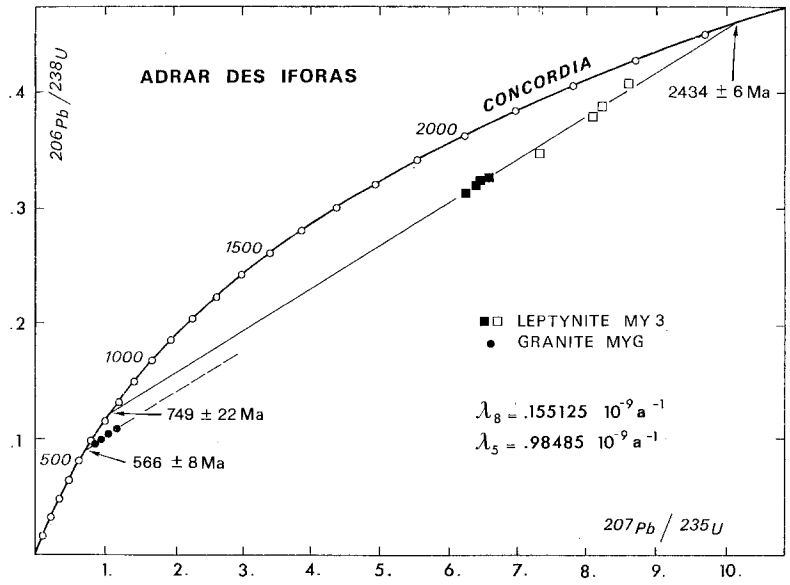

Fig. 6. Concordia diagram $^{207}Pb/^{235}U$ vs $^{206}Pb/^{238}U$ for zircons of the leptynite MY3 (Iforas granulitic unit); (■) magnetic zircon fractions; (□) non magnetic zircon fractions; (●) coarse zircon fractions from the granite MYG are plotted for comparison. The 749–2,434 Ma chord is a linear regression line of the zircon samples from the leptynite MY3

were extracted from the sub-alkaline leptynite MY3 (see location Fig. 2). These crystals are also characterized by rare little black inclusions and an extensive development of micro-cracks.

The experimental points of zircons MY3 are plotted in a Concordia diagram (Fig. 6), where they define a linear array, the magnetic zircon fractions being more discordant than the non-magnetic ones. The upper and lower intercept ages, are respectively 2,434 ± 6 Ma and 749 ± 22 Ma. These values are interpreted, on the basis of zircon U·Pb data on the In Ouzzal granulitic unit and of recent measurements by Rb – Sr and Sm – Nd methods on whole rocks and minerals (Lancelot et al. 1975, 1976; Lancelot 1975; Allègre and Ben Othman 1980). The results clearly indicate that in the Hoggar, 3,000–3,300 Ma-old continental material underwent a granulite facies metamorphism 2,120 ± 20 Ma ago. Assuming that the granulite facies metamorphism episode in the Iforas granulitic unit is the same as that which affected the In-Ouzzal basement 2,120 Ma ago (Fig. 1), we propose a multistage model (Allègre et al. 1974) with two episodic lead losses to explain the observed trend in the Concordia diagram for the zircons MY3. In this model, after the zircon crystallization 3,000–3,300 Ma ago, a first episodic lead loss occurred 2,120 Ma ago, during a granulite facies metamorphism episode, but the U·Pb systems of the zircons were not completely reset during this event. A second episodic loss of radiogenic lead affected all these zircons during Pan African orogeny. The model is a possible explanation of the 749 ± 22 Ma age provided by the lower intercept, an age which is not geologically significant in the studied area. Furthermore this model is in agreement with other U·Pb data reported in this paper: quartzites M578 and IF9, ultramylonite MY7. In a multistage model, with two episodic lead losses (Allègre et al. 1974; Gebauer and Grünenfelder 1979) the behavior of the U·Pb system of zircons can lead to quasi-linear arrays of data points with geologically meaningless intercept ages. We denote by T_u the upper and by T_l the lower intercepts. If T_0, T_1 and T_2 correspond respectively to the ages of zircon crystallization, and first and second lead losses, then $T_1 < T_u < T_0$ and

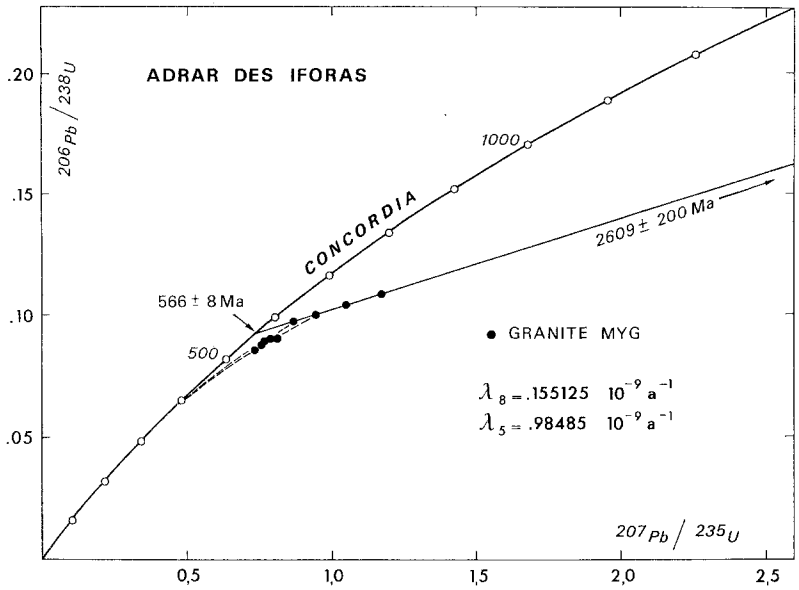

Fig. 7. Concordia diagram $^{207}Pb/^{235}U$ vs $^{206}Pb/^{238}U$ for zircons of the granite MYG. The 566–2,609 Ma chord is a linear regression line of the coarse zircon fractions from the granite MYG

$T_2 < T_t < T_1$. Thus, in this model, the 2,434 Ma age is not the age of crystallization of the leptynites but an intermediate age between the real age of zircons crystallization and the age of the granulite facies metamorphism (2,120 ± 20 Ma).

IV.3 Quartzite IF9 of the Iforas Granulitic Unit

Clear, pink, rounded (drop-shaped) zircons with very little black inclusions were extracted from the quartzite IF9 (Fig. 4). These crystals have the same pseudofaces found in M578 and MY3 samples, which is indicative of a high pressure metamorphic episode (Lasnier 1977; Hope 1966). U – Pb isotopic analyses of zircons from the quartzite IF9, plotted on a Concordia diagram (Fig. 5) show a pattern which can be explained by a multistage model similar to that used for the leptynite MY3. Initially, the quartzite contained 3,100–3,300 my-old detrital zircons. The first strong episodic loss of radiogenic lead occurred 2,120 Ma ago during granulite facies metamorphism, and the second loss is related to the thermal-tectonic Pan African event (550–650 Ma) in the Iforas. During granulite facies metamorphism, recrystallization of zircons occurred which is demonstrated by the presence of inherited cores and drop shapes of zircon crystals with pseudo-faces. After the first disturbance, the discordancy of zircon IF9 was probably more variable than these of leptynite MY3. The finer-size fractions, with greather U content (Silver and Deutsch 1963), show a younger apparent $^{207}Pb/^{206}Pb$ age of 2,350 Ma, in comparison with the coarser fraction, which is characterized by a lower U content and an older apparent $^{207}Pb/^{206}Pb$ age of 2,450 Ma.

V Deformation and Radiochronology

This part of the study includes:
– the U/Pb dating on zircons of a late Pan African calc-alkaline granite (sample MYG), intruded the western margin of the Iforas unit (Fig. 2) and slightly deformed by the NO 10 trending shear zone;
– the U/Pb systematics on zircons broken and rolled in the ductile matrix of the ultramylonite MY7 which presents the same chemical composition that the undeformed leptynite MY3;
– the $A^{39} - A^{40}$ dating on K feldspars from three samples collected along one cross-section of the shear zone (Fig. 2) and following the gradient of strain.

V.1 The U – Pb Age of a Late Pan-African Granite Deformed by the Shear Zone

The zircons from granite MYG are euhedral (Fig. 4) and many crystals have inherited cores (Fig. 8). Most of the zircon crystallized with Sn form (with $1 < n < 8$), which indicates low temperatures of formation ranging from 650° to 700° C (Pupin 1980). However, a few crystals show Q_1, Q_2, P_1, P_2 forms. The U – Pb data, plotted in a Concordia diagram (Fig. 7) also clearly indicate the presence of zircons with inherited cores. The cores represent the remnants of ancient zircons which were not entirely melted during the partial melting process which gave rise to the granite MYG. Note the case of several newly-formed zircons, growing upon a single inherited core (Fig. 8). Cases of granites (s.l.) and acid orthogneisses, with inherited zircons or zircons with inherited cores are well known (Davis et al. 1968; Grauert and Hofmann 1973; Gulson and Rutishauer 1976; Pankhurst and Pidgeon 1976; Pidgeon and Aftalion 1978; Pin 1981). For the granite MYG, in a Concordia diagram, the experimental points define two trends (Fig. 7) related to the size, the magnetism, and, of course, the U-content of zircon fractions. Coarse-grained zircons with sizes ranging from 200 μ to 100 μ define a linear array with 566 ± 8 Ma and 2,609 ± 200 Ma intercepts ages. Small zircons ranging in size from 100 μ to 63 μ, define a curve which is tangential in its upper part with the discordia line of the coarse zircons. This pattern is interpreted as follows:

a) 566 ± 8 Ma ago, there was a partial melting of the leptynites or of rocks with the same isotopic signature (i.e. rocks with 3,100–3,300 Ma Sm – Nd model age and affected by 2,120 Ma-old granulite facies metamorphism). Rem-

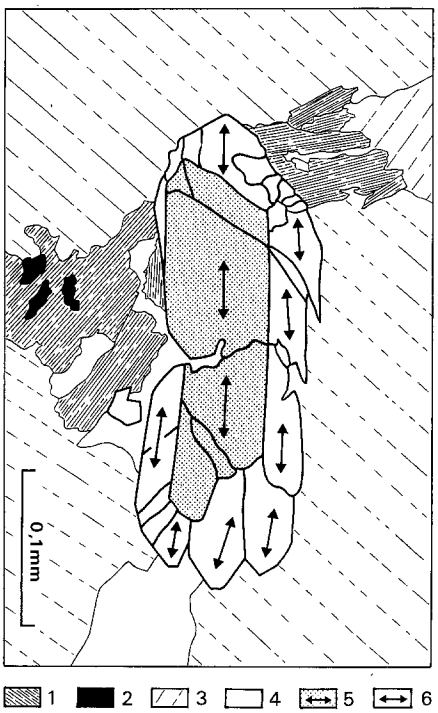

Fig. 8. Schematic drawing after a photograph of a zircon from the granite MYG showing epitaxic overgrowths on an inherited core. The line indicates the orientation of the C axis in each crystal. (1) biotite; (2) K-feldspar; (3) iron oxyde; (4) quartz; (5) inherited core; (6) newly formed zircons

nants of incompletely dissolved zircons with their U–Pb system not entirely reset, were present in the granitic melt. A new generation of zircons then crystallized from the melt either as overgrowths on the inherited zircons or as completely new crystals. Then, experimental points define a mixing line, whose lower intercept with the Concordia curve at 566±8 Ma, provides the age of partial melting and crystallization of the newly-formed zircons. The poorly defined upper intercept of 2,609±200 Ma resulting from the extreme discordancy of experimental points) indicates the U–Pb apparent age of the material which underwent partial melting, i.e. rocks crystallized 3,000–3,300 Ma ago and affected by the 2,120 Ma old granulite facies metamorphism.

b) After 566±8 Ma, a low radiogenic lead-loss occurred for the U-rich small-sized zircon fractions. Consequently, some experimental points plot a curve under the mixing line previously defined (Fig. 7). As the granite MYG is slightly deformed by the NO 10 trending shear zone, the U–Pb dating of this granite provide an upper limit of 566±8 Ma for the age of the mylonitic episod.

V.2 U–Pb Zircon Geochronology of the Ultramylonite MY7

Zircons extracted from the ultramylonite MY7 (Fig. 4) show the clear imprint of superficial corrosion phenomena and a reduction of diameter in comparison with those of the undeformed leptynite MY3. As a matter of fact, the breakage of zircons during the studied tectonic episode provides abundant crystal fragments of diameters ranging from 50 to 80 μ (Boullier 1980b). U–Pb analysis has been carried out on small sample weights (ranging from 0.16 to 0.49 mg), with the "direct loading" method, without chemical separation of the uranium and the lead from the Zr SiO_4 matrix (Lancelot et al. 1973–1976; Lancelot 1975).

Plotted on the Concordia diagram, the experimental points are slightly discordant (Fig. 9) and are quite comparable with those of zircons extracted from the quartzite M578. They define a linear array whose upper intercept with the Concordia curve provides an age of 2,120±7 Ma. This pattern, on the one hand, confirms the occurrence of a major granulitic event in the pre Pan-African basement of the Hoggar and the Iforas (Lancelot et al. 1973–1976) and on the other hand, indicates that the tectonic event which produced the ultramylonite MY7, did not induce a clear opening of the U·Pb system of the broken zircons in the ultramylonite. Deformed and undeformed leptynite (samples MY7 and MY3) present the same chemical composition (Boullier, unpublished data), nevertheless the $^{207}Pb/^{206}Pb$ ratios of their zircons are distinct. To interpret this fact, we note that veins of pegmatoid leucosomes are common in leptynites of the Iforas granulitic unit. These veins are contemporaneous with the granulite event and we assume that the newly-formed zircons without inherited core crystallized preferentially in theses, 2,120 Ma ago. Then this age will be found for zircons of an ultramylonite, derived by tectogenesis under low temperature conditions, from a leptynite where the veins of pegmatoid leucosome were significant. We note, here, the problem of rock material deplacements in the shear zone itself and the interest of radiochronological study on zircons microsamples or single zircons in this case (Lancelot et al. 1976).

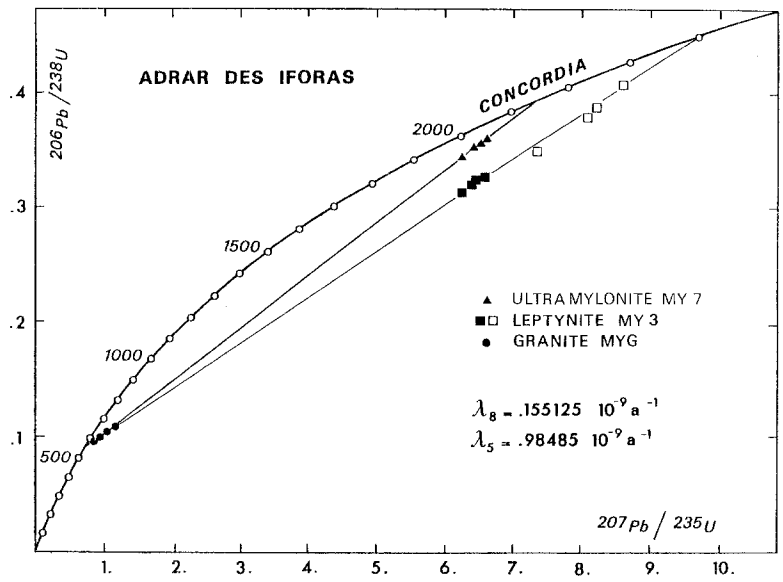

Fig. 9. Concordia diagram $^{207}Pb/^{235}U$ vs $^{206}Pb/^{238}U$ for zircons of the ultramylonite MY7 (▲). Coarse zircon fractions from the deformed granite MYG (●) and zircon fractions from the undeformed leptynite MY3 (■, □) are plotted for comparison

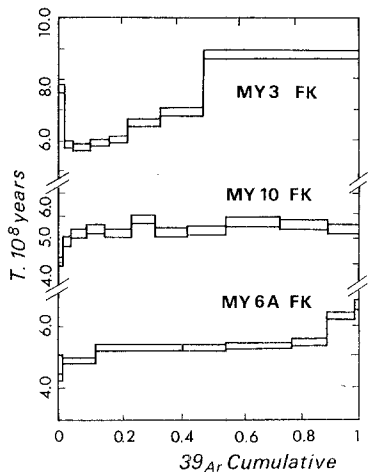

Fig. 10. $^{40}Ar/^{39}Ar$ age-spectrum plot for the MY3, MY10 and MY6 K feldspars. Mean plateau ages of 525 ± 8 Ma and 535 ± 6 Ma can be respectively defined for deformed samples MY10 and MY6

V.3 $A^{39}-A^{40}$ Dating of the Deformation

Three K-feldspars were analyzed with the $^{40}Ar/^{39}Ar$ method, using a stepwise heating technique. Samples were chosen according to their state of strain: we selected K-feldspar from a leptynite which did not show any evidence of deformation (MY3); the second sample was a mylonite which suffered moderate deformation (MY10); the third sample (MY6) was an ultramylonite from the center of the shear zone.

The age spectrum of the MY3 feldspar (Fig. 10) shows the usual partial loss (Berger 1975; Maluski 1978). Apparent ages related to the Argon release of low-temperature locales yield a minimum age. Maximum ages are only reached in high temperatures. Although the sample MY3 does not show any deformation, the trend of this age-spectrum demonstrates the influence of a disturbing phase which has acted on the retentive and less-retentive locales in the K-feldspars. It results in a differential loss of Argon which is much more significant for non-retentive locales than for retentive ones. Due to this loss, the maximum age obtained during the fusion of the sample is probably geologically meaningless ($\simeq 900$ Ma) with no clear relation to any thermal or tectonic event. We shall compare better ages of low temperature steps with other ones.

Spectrum of the K-feldspar MY10 shows homogeneous apparent ages. Only the first three steps give lower ages (570, 450, and 495 Ma). The average of the other steps is 525 ± 8 Ma. These data yield an age of 532 ± 5 Ma with a $^{40}Ar/^{36}Ar$ versus $^{39}Ar/^{36}Ar$ diagram. The age of direct fusion is 535 ± 5 Ma.

The spectrum of the K-feldspar MY6A also shows homogeneous apparent ages. Only the first and the last two step-ages are very scattered, which is a result of the very small amount of ^{39}Ar released. As a consequence, they can be discarded, as proposed by Lanphere and Dalrymple (1971). The average value of ages is 535 ± 6 Ma. With the $^{40}Ar/^{36}Ar$ versus $^{39}Ar/^{36}Ar$ diagram these data give an age of 439 ± 5 Ma.

Age spectra of deformed samples (MY10 and MY6A) give concordant ages: 532 and 539 Ma (Fig. 10). The presence of a plateau age of about 535 Ma shows that all of the locales lost their radiogenic argon during a disturbing event which occurred after their first closure. If we assume that all of the locales had a closed-system behavior after this event, the age of 535 Ma can be interpreted as the final age of the tectonic phase which was responsible for the deformation of the leptynites and of the granite. The behavior of the MY3 K-feldspar is more peculiar: low temperature ages are higher than those of the other two feldspars. In the area where this sample comes from, the disturbing effect of tectonics was not strong enough to reset totally the locales with low activation energy. Only a partial loss occurred from these locales, which yield an intermediate age with no clear significance. This result is very similar to those obtained in a progressively deformed area in Corsica (Maluski 1978) and in disturbed hercynian zones in the Pyrénées (Albarède 1978). It confirms that K-feldspars can begin to suffer a loss in a very slightly tectonized area, and can be completely reset when deformation is strong enough to allow a complete release of radiogenic argon in all locales. Results from deformed K-feldspar

allow us to confirm that the time emplacement of the granite (566 ± 8 Ma) was anterior to the main mylonite episode which ended 535 ± 6 Ma ago.

VI Conclusions

(1) The western mylonitized margin of the Iforas granulite unit (Mali) is a NO 10 trending shear zone, which cross-cuts both the banding of the granulite and a postkinematic Pan-African calc-alkaline granite. The gradient of strain in the shear zone is described by its mineralogical consequences. For zircon behavior, the main observed feature is the decrease of grain size toward the center of the shear zone. Under postprotomylonitic conditions, cracks appeared in the zircons, and then as strain increased, the grain size decreased until an equilibrium grain size of 30 μ was reached. The brittle behavior of zircon is independant of the initial grain size of the crystals in the undeformed sample.

(2) In the NW part of the Hoggar (Algeria), previous U – Pb dating of zircons (Lancelot et al. 1973, 1976; Lancelot 1975) indicated that a major granulite facies metamorphic event occurred 2,120 Ma ago. The grain-by-grain analysis of zircons with inherited core demonstrated that these zircons were derived from an old continental crust, formed 3–3.3 Ga ago. Taken in the granulite terranes of the Iforas and the In Ouzzal units samples of two quartzites and an undeformed alkaline leptynite confirm that a 2,120 Ma granulite facies metamorphism is a characteristic of the Precambrian basement of the Hoggar and the Adrar des Iforas. No traces of a Kibarian event, at 1,000 Ma, can be recorded in these rocks. Zircons without inherited cores from the quartzite (M578) of the In Ouzzal unit, show a normal discordancy with a crystallization age of 2,115 ± 6 Ma. On the otherhand, zircons extracted from the quartzite (IF9) and from the MY3 undeformed alkaline leptynite (MY3) of the Iforas unit, show inherited core, and the U – Pb data suggest the following multistage model:
- inherited zircons from a basement 3 to 3.3 Ga old;
- a strong episodic loss of radiogenic lead induced by granulite facies metamorphism at 2,120 Ma;
- a secondary episodic loss of radiogenic lead during Pan-African orogeny.

(3) A calc-alkaline granite (MYG), emplaced after the main Pan-African thermo-tectonic event, intruded the Iforas granulitic unit and was deformed by the shear zone of the western margin of this unit. This granite is the first example of a Pan-African magmatic rock with inherited core in the zircons. U – Pb data indicate a partial melting of the leptynites (or of rocks with the same Pb isotopic signature) 566 ± 8 Ma ago, which gave rise to the granite MYG. This age also provides an upper limit for the dating of the mylonitic event.

(4) K-feldspars were extracted from three samples of sub-alkaline leptynites collected by following the gradient of strain in the shear zone. These feldspars were analyzed by the $Ar^{39} - Ar^{40}$ method, using a stepwise heating technique. The high-temperature steps yield ages ranging from 535 ± 5 Ma to 539 ± 5 Ma for a mylonite (MY10) and an ultramylonite (MY6A). These data indicate that the main mylonite episode ended at 535 ± 6 Ma. The undeformed sample (MY3) yields an age of 900 Ma, which is without apparent geological significance.

(5) Plotted on a Concordia diagram, the U – Pb data on zircons from an ultramylonite (MY7) yield a pattern similar to that obtained for the quartzite (M578) and the undeformed leptynite (MY3). This result indicates that the tectonic event did not induce a clear opening in the U – Pb system of the zircons, even when these crystals were broken and rolled in the ductible matrix of the ultramylonite. Zircons show a brittle behavior and are not subject to dynamic recrystallization at the low-temperature conditions which prevailed in this case. The different responses of the two chronometric systems ($Ar^{39} - Ar^{40}$ on K-feldspar and U – Pb on zircon) to the same tectonic event at low temperature should be emphasized. From this study, we assume that these complementary chronometers can be used in similar cases, even on ultradeformed samples, to study the radiochronology of brittle deformation at low temperature and of deformed country rocks. It should also be noted that the study of small samples is of particular interest in a strongly deformed area where rock material deplacements are common in the shear zone itself.

Acknowledgements. We are indebted to R. Caby for helpful discussions and for the sampling of the quartzite M578. This work has been carried out with the financial support of the C.N.R.S., L.P. "Centre Géologique et Géophysique", the C.N.R.S., L.A. 266 and the A.T.P. Géochimie (Contract n° A651 35.23).

Appendix: Sample Description

MY3: Undeformed sub-alkaline leptynite; granoblastic texture. Mineralogical composition: mesoperthitic feldspar; partly sericitized plagioclase (An 20) containing tiny crystals of calcite; quartz with ondulatory extinction, and large subgrain; pale green clinopyroxene surrounded by bluish-green amphibole; large brownish-green primary amphibole with bluish rim; ilmenite-magnetite aggregates surrounded by green biotite; apatite; zircon; allanite; rutile.

MY10: Mylonitic sub-alkaline leptynite. Mineralogical composition: fractured fragments of mesoperthitic feldspar and partly sericitized plagioclase (≃An 20) which are recrystallizing on their margin into minute equant crystals of albite; syntectonic bluish green amphibole; ribbons of quartz recrystallized in equant grains; apatite; ilmenite-magnetite aggregates rimmed by leucoxene; zircon.

MY6 and MY7: ultramylonitic sub-alkaline leptynite. Mineralogical composition: fragments of mesoperthitic feldspar; in very fine grained matrix: microcline and albite; ribbons of quartz recrystallized in equant grains; green biotite; chlorite; calcite; opaque minerals with leucoxene; zircon; apatite.

MYG: Deformed calc-alkaline granite. Broken fragments of epidiomorphic crystals of feldspars: perthitic microcline and partly sericitized zoned oligoclase (≃An 25) with deformed albite twins; quartz with mortar structure (relicts of porphyroclasts within a mosaic of equant crystals); two generations of greenish-brown biotite: large deformed crystals often chloritized and microcrystalline grains in strings with recrystallized quartz or alkali feldspar; secondary muscovite; clinozoisite; apatite; zircon; allanite.

IF9: Granulitic feldspathic quartzite with a granoblastic texture. Large crystals of quartz; garnet; mesoperthitic feldspar; rutile partly retromorphosed into ilmenite and brown biotite; phengite; zircon.

M578: Granulitic quartzite; granoblastic texture. Large crystals of quartz with inclusions of rutile needles; prismatic rutile with sphene; zoisite; cummingtonite, muscovite and calcite replacing clinopyroxene; apatite; zircon; opaque minerals.

References

Abbott JT (1972) Rb – Sr study of isotopic redistribution in a Precambrian mylonite-bearing shear zone, Northern Front Range, Colorado. Geol Soc Am Bull 83:487–494

Albarede F (1971) Etude quantitative de l'histoire géologique d'une région polytectonique à l'aide des modèles complexes de comportement géochimique des systèmes radiométriques U/Pb. Exemple d'application: cas des Alpes Suisses. Thesis Univ Paris VI

Albarede F, Feraud G, Kaneoka I, Allegre CJ (1978) $^{39}Ar-^{40}Ar$ dating: the importance of K-feldspars on multi-mineral data of polyorogenic areas. J Geol 86:581–598

Allegre CJ, Albarede F, Grünenfelder M, Koppel V (1974) $^{238}U/^{206}Pb$, $^{235}U/^{207}Pb$, $^{232}Th/^{208}Pb$ zircon geochronology in Alpine and non Alpine environment. Contrib Mineral Petrol 43:163

Allegre CJ, Ben Othman D (1980) Nd isotopic relationship in granitoid rocks and continental crust development: a chemical approach to orogenesis. Nature 286:335–342

Berger GW (1975) $^{40}Ar-^{39}Ar$ step heating of thermally overprinted biotite, hornblende and potassium feldspar from Eldora Colorado. Earth Planet Sci Lett 26:387–408

Bernard-Griffiths J (1975) Essai sur la signification des âges au strontium dans une serie métamorphique. Le Bas Limousin (Massif Central français). Univ Clermont-Ferrand Thesis

Bertrand JM, Bertrand-Sarfati J, Caby R, Moussine-Pouchkine A (1980) Upper Proterozoic correlations between the West African craton and the panafrican mobile belt in Algeria and Mali. In: Kratz O (ed) Correlation du Precambrien – I.U.G.S., Acad Sc URSS, Leningrad

Black R, Caby R, Moussine-Pouchkine A, Bayer R, Bertrand JM, Boullier AM, Fabre J, Lesquer A (1979) Evidence for late Precambrian plate tectonics in West Africa. Nature 278:(5701)223–227

Boullier AM (1980a) Charriages et déformations del'unité granulitique des Iforas au course de l'orogénèse pan-africaine. Rev Géol Dyn Géogr Phys 21:(5)377–382

Boullier AM (1980b) A preliminary study on the behaviour of brittle minerals in a ductile matrix: example of zircon and feldspar. J Struct Geol 2:211–217

Boullier AM, Davison I, Bertrand JM, Coward M (1978) L'unité granulitique des Iforas: une nappe de socle d'âge panafricain précore. Bull Soc Géol Fr 7:(XX, 6)877–882

Boullier AM, Gueguen Y (1975) S.P. mylonites: origin of some mylonites by superplastic flow. Contrib Mineral Petrol 50:93–104

Caby R (1970) La chaîne pharusienne dans le Nord-Ouest de l'Ahaggar (Sahara central, Algérie); sa place dans l'orogénèse du précambrien supérieur en Afrique. Thèse d'Etat, Univ Montpellier, 336 p

Caby R, Boullier AM (1977) Le môle granulitique des Iforas (Mali). Nature et comportement au cours de l'orogenèse panafricaine. 5ème réunion ann. Sci. Terre, Rennes, p 124

Cogez P, Sulmont N (1978) Etude de la discrimination de masse au cours des analyses de plomb dans la source thermoionique d'un spectrométre de masse. Projet industriel. Ec Sup chim, Montp, 94 p

Collerson KD (1974) Descriptive microstructural terminology for high grade metamorphic tectonites. Geol Mag (III)4:313–318

Davis GL Hart SR, Tilton GR (1968) Some effects of contact metamorphism on zircon ages. Earth Planet Sci Lett 5:27–34

De la Boisse H, Lancelot JR (1977) A propos de l'évènement à 1000 M.a. en Afrique Occidentale. 1: le granite de Bourré. Compt Rend Somm Soc Géol Fr 4:223–226

Desportes A, Lancelot JR (1975) Etude au microscope à balayage et à la microsonde de la répartition des éléments dans les zircons et dans leurs inclusions. 3ème Réunion ann. Sci Terre (Montpellier) p 129

Gastil RG, Delisle M, Morgan JR (1967) Some effects of progressive metamorphism on zircons. Bull Geol Soc Am 78:879–906

Gebauer D, Grünenfelder M (1978) Low temperature recrystallization of zircon as a cause of discordant U – Pb data. IV Intern Conf Geoch Cosmoch Isot Geol 133:135

Gebauer D, Grünenfelder M (1979) U – Th – Pb dating of minerals. In: Lectures in isotope geology. Springer, Berlin Heidelberg New York, pp 105–131

Grauert B, Hofmann A (1973) Old radiogenic lead components in zircons from the Idaho batholith and its metasedimentary aureole. Carnegie Inst Year Book 72:Dep Terr Magn 297–299

Grünenfelder M (1963) Heterogenität akzessorischer zirkone und die petrogenetische Deutung ihrer Uran/Blei Zerfallsalter. Schweiz Min Petr Mitt 43:235

Grünenfelder M, Hanson GN, Brunner GO, Eberhard E (1968) U – Pb discordance and phase unmising in zircons. Bull Geol Soc Am 77:1202

Gulson LB, Rutishauser H (1976) Granitization and U – Pb studies of zircons in the Lauterbrunnen crystalline complex. Geoch J 10:13–23

Higgins MW (1971) Cataclastic rocks. Geol Surv Prof Paper 687:97

Hoppe G (1966) Zirkone aus granuliten. Bern Deutsch Ges Geol Wiss B Miner Lagerstat Tenk II 1:47–81

Jaffey AH, Flynn KF, Glendenin LE, Bentle EC, Essing AM (1971) Precision measurements of half lives and specific activities of ^{235}U and ^{238}U. Phys Rev CA 1889–1906

Krogh TE (1973) A low contamination method for hydrothermal decomposition of zircon and extraction of U and Pb for isotopic age determinations. Geoch Cosmoch Acta 37:585–494

Lancelot JR (1975) Les systèmes U/Pb, chronomètres et traceurs de l'évolution des roches terrestres. Univ Paris VII Thesis, 280 pp

Lancelot JR, Vitrac A, Allegre CJ (1975) Datation U – Th – Pb des zircons grain par grain par dilution isotopique, conséquences géologiques. CR Acad Sci Paris 277:2117–2120

Lancelot JR, Vitrac A, Allegre CJ (1976) Uranium lead isotopic dating with grain by grain zircon analysis: a study of complex geological history with a single rock. Earth Planet Sci Lett 29:357–366

Lancelot JR, De la Boisse H, Joyer P (1979) Progrès analytiques en spectrométrie de masse pour la datation des zircons par la méthode U – Pb. 7éme Réun Ann Sci Terre Lyon Soc Géol France p 274

Lanphere MA, Dalrymple GB (1971) A test of the $^{40}Ar/^{39}Ar$ age spectrum technique on some terrestrial materials. Earth Planet Sci Lett 12:359

Lasnier B (1977) Persistance d'une série granulitique au coeur du Massif Central français (Haut Allier): les termes basiques, ultrabasiques et carbonatés. Thèse Univ Nantes, 351 pp

Leyreloup A (1974) Evolution plurifaciale du métamorphisme granulitique dans les paragneiss archéens du môle In Ouzzal (Hoggar, Sahara algérien). 2ème Réun Ann Sci Terre (Nancy), p 261

Ludwig KR (1980) Calculation of uncertainties of U – Pb isotope data. Earth Planet Sci Lett 46:212–220

Maluski H (1978) Behaviour of biotites, amphiboles, plagioclases and K-feldspars in response to tectonic events with the $^{40}Ar-^{39}Ar$ radiometric method. Example of Corsica granite. Geochim Cosmochim Acta 42:1619–1633

Pankhurst RJ, Pidgeon RT (1976) Inherited isotope systems and the source region prehistory of early Caledonian granites in the Dalradian series of Scotland. Earth Planet Sci Lett 31:55–68

Pidgeon RT, O'Neil JR, Silver LT (1966) Uranium and lead isotopic stability in a metamict zircon under experimental hydrothermal conditions. Sciences 154:1538–1540

Pidgeon RT, Aftalion M (1978) Inherited zircon U – Pb system as indicators of granite souce rocks in the British Caledonides. IV Int Conf Geochron Cosmochron Isot Geol Aspen 335–336

Pin C (1981) Old inherited zircons in two synkinematic variscan granitoids: the "granite du Pinet" and the "orthogneiss de Marvejols" (southern french Massif Central). N Jb Mineral Abh 142:27–48

Pupin JP (1980) Zircon and granite petrology. Contrib Mineral Petrol 73:207–220
Quinquis M, Audren Cl, Brun JP, Cobbold PR (1978) Intense progressive shear in Ile de Groix blueschists and compatibility with subduction or obduction. Nature 273:(5657)43–45
Sibson RH (1977) Fault rocks and fault mechanisms. J Geol Soc London 133:(3)191–214
Silver LT, Deutsch S (1963) Uranium lead variations in zircons. A case study. J Geol 71:721–758
Steiger RH, Jäger E (1977) Subcommission on geochronology. Convention of the use decay constants in geo and cosmochronology. Earth Planet Sci Lett 36:359–362
Tilton GR (1960) Volume diffusion as a mechanism for discordant lead ages. J Geophys Res 65:2933–2945
Ulrych TJ (1963) Discordant lead-uranium ages due to continuous loss of lead. Nature 200:561–562
Wasserburg GJ (1963) Diffusion processes in lead-uranium systems. J Geophys Res 68:4823–4846
Wetherill GW (1956) Discordant uranium-lead ages. I Trans Am Geophys Union 37:320–326

Accepted February 16, 1983